LSST survey: millions and millions of quasars

Željko Ivezić

Department of Astronomy, University of Washington,
Box 351580, Seattle, WA 98195-1580, USA
email: ivezic@astro.washington.edu

Abstract. The Large Synoptic Survey Telescope (LSST), the next-generation optical imaging survey sited at Cerro Pachon in Chile, will provide hundreds of detections for a sample of more than ten million quasars with redshifts up to about seven. The LSST design, with an 8.4m (6.7m effective) primary mirror, a 9.6 sq. deg. field of view, and a 3.2 Gigapixel camera, will allow about 10,000 sq. deg. of sky to be covered twice per night, every three to four nights on average, with typical 5-sigma depth for point sources of $r=24.5$ (AB). With about 1000 observations in $ugrizy$ bands over a 10-year period, these data will enable a deep stack reaching $r=27.5$ (about 5 magnitudes deeper than SDSS) and faint time-domain astronomy. The measured properties of newly discovered and known astrometric and photometric transients will be publicly reported within 60 sec after closing the shutter. In addition to a brief introduction to LSST, I review optical quasar selection techniques, with emphasis on methods based on colors, variability properties, and astrometric behavior.

Keywords. surveys, galaxies: active, quasars: general, stars: variables, stars: statistics

1. Introduction

The selection of large samples of active galactic nuclei, including quasars as their high-luminosity tail, is required in many astrophysical areas, such as galaxy evolution, black hole growth, and the large-scale structure of the universe. The available quasar samples have increased by over two orders of magnitude in less than two decades and this rapid progress is expected to continue (for example, simulations predict that LSST will deliver a sample of about 10 million quasars; see Section 3.1). Here I briefly review optical quasar selection methods based on SDSS data and discuss how they will be improved with the aid of more precise time-resolved photometry expected from LSST. My main sources, where more detailed information about LSST and AGN/quasar science with LSST data can be found, include the so-called LSST overview paper (Ivezić *et al.* 2008) and the LSST Science Book (LSST Science Collaboration 2009).

2. Finding quasars with SDSS

The similarity of unresolved quasars to stars in optical imaging surveys poses a difficulty in their identification. Quasars can be reliably identified by their spectra, and the SDSS provided a spectroscopically complete survey to $i < 19$ with ∼106,000 quasars (Schneider *et al.* 2010). This is the largest homogeneous quasar sample with high-quality optical spectra assembled to date (Pâris *et al.* 2012 recently reported an additional ∼74,000 objects selected with selection criteria modified to enable the Lyman-α forest analysis). These objects were selected as quasar candidates using colors measured from the $ugriz$ SDSS imaging data, and also using radio continuum 20 cm data from the FIRST survey (Becker *et al.* 1995). After SDSS collected enough multi-epoch imaging data, it was demonstrated that photometric variability-based selection is even more
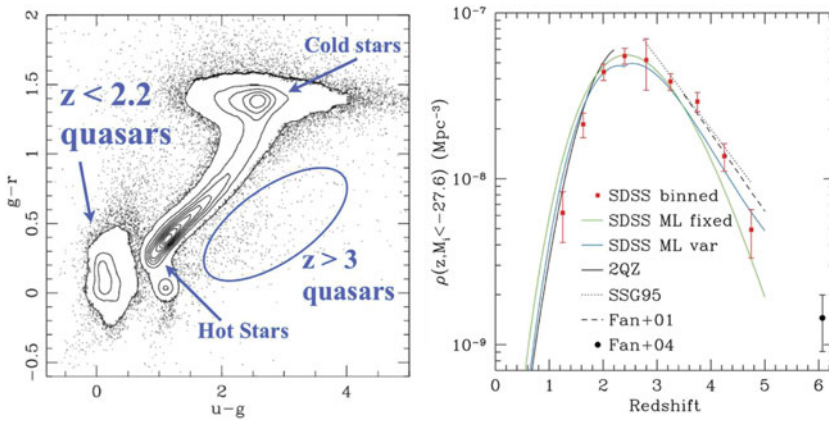
Figure 1. The left panel illustrates the color-based selection method for quasar candidates. Essentially, the algorithm selects all sources whose colors place them outside the main stellar locus, seen in the middle of the panel. Quasars with redshifts below 2.2 have distinctively blue $u - g$ colors. The right panel shows the variation of volume number density of luminous quasars. The local maximum at about $z = 2.4$ is clearly visible. Adapted from Richards *et al.* (2006).

efficient than color-based selection. These two selection methods are briefly summarized here.

2.1. *Color selection of quasar candidates*

A small fraction of SDSS sources unresolved in imaging data were automatically targeted as quasar candidates for spectroscopic followup (Richards *et al.* 2002). The quasar targeting algorithm selects all point sources with $15 < i < 19.1$ (i is the apparent magnitude in the SDSS i band) whose colors place them outside the main stellar locus (it is a bit more complicated than this – for details please see figure 1 in Richards *et al.* 2002). For quasars at redshifts below about two, the most discriminatory color is the $u - g$ color: compared to stars of the same visual color (e.g., the $g - r$ color), quasars show an excess of ultraviolet flux in the u band and thus have bluer $u - g$ colors (see the left panel in Figure 1); this method is often called the UV-excess selection. The colors of quasars at higher redshifts are typically significantly different from stellar colors. A thorough analysis of the colors of quasars in the SDSS photometric system was presented in Richards *et al.* (2001). In addition, all unresolved sources from the same magnitude range that are within 2 arcsec of a FIRST radio detection are also targeted (for analysis of these radio quasars, see Kimball *et al.* 2011 and references therein). Some quasars were also targeted fortuitously via the algorithms for selecting galaxies (Strauss *et al.* 2002). The completeness of the resulting quasar sample is above 90% (the confirmed fraction of all quasars within the adopted flux limits and within the surveyed area) and the efficiency of color selection is about 65% (that is, about 35% of selected quasar candidates turned out not to be quasars). This homogeneously selected sample spans a large redshift range (there are 56 quasars at redshifts beyond 5 in the Schneider *et al.* sample) and has enabled numerous quasar studies. For example, the peak in the comoving volume number density of luminous quasars (dominated by type I objects) is now reliably and precisely determined (see the right panel in Figure 1), and the luminosity functions of quasars and AGN galaxies (selected using emission line strengths) appear mutually consistent despite grossly different selection procedures (Hao *et al.* 2005). We note that several hundred candidate type II quasars (high-luminosity analogs of type 2 Seyfert galaxies) were found in the SDSS spectroscopic survey of galaxies (Zakamska *et al.* 2003, 2004).
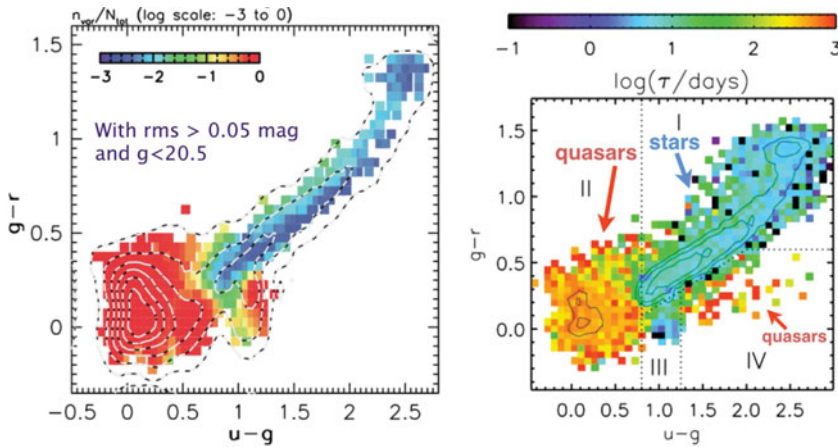
Figure 2. The left panel shows the fraction of point sources with $g < 20.5$ from SDSS Stripe 82 dataset that are variable (the root-mean-square variation of at least 0.05 mag; adapted from Sesar *et al.* 2007). The two regions where essentially all point sources are variable correspond to low-redshift quasars ($u - g \sim 0$) and RR Lyrae stars ($u - g \sim 1$). The right panel shows the median characteristic timescale τ for all variable point sources in SDSS Stripe 82 dataset that are well described by the damped random walk model, as a function of $u - g$ and $g - r$, following the legend at the top (adapted from MacLeod *et al.* 2011).

The relatively simplistic color-based selection algorithm employed by the original SDSS spectroscopic target selection pipeline has been significantly improved using modern data mining and machine learning methods. For example, Richards *et al.* (2009) introduced a kernel density estimator and a non-parametric Bayesian classification method, and Bovy *et al.* (2012) introduced a Gaussian mixture model to recognize quasar candidates. These methods have yielded large samples of candidates (of order a million) and with improved completeness and efficiency tradeoff; Richards *et al.* (2009) reported efficiency of up to 97% while maintaining fairly high completeness levels above 70%. More details about the performance of these modified selection algorithms are available in Pâris *et al.* (2012) and Ross *et al.* (2012).

2.2. *Variability selection of quasars*

Quasars are variable sources with optical amplitudes of several tenths of a magnitude for time scales longer than a few months, and this behavior can be used for their selection (Hawkins & Veron 1995; Ivezić *et al.* 2003). Sesar *et al.* (2007) showed using SDSS Stripe 82 data (a $\sim$300 deg^2 equatorial region imaged about 60 times) that practically all quasars spectroscopically confirmed by SDSS are also variable in SDSS imaging data (see left panel in Figure 2), and Kozłowski *et al.* (2010) demonstrated that variability can be used to separate quasars from most variable stars even in the dense stellar environments of the Magellanic Clouds.

A number of studies used SDSS light curves for close to 10,000 quasars from Stripe 82 to quantify the structure function for quasar variability (Ivezić *et al.* 2004; MacLeod *et al.* 2010; Schmidt *et al.* 2010; Butler & Bloom 2011; Palanque-Delabrouille *et al.* 2011). The structure function as a function of time lag Δt, SF(Δt), as defined in recent quasar studies, is equal to the standard deviation of the distribution of the magnitude difference $m(t_2) - m(t_1)$ evaluated at many different times t_1 and t_2, such that time lag $\Delta t = t_2 - t_1$ (and divided by $\sqrt{2}$ because of differencing). The structure function is directly related to the autocorrelation function, which makes a Fourier pair with the power spectral density function (PSD). When the structure function SF $\propto (\Delta t)^{\alpha}$, then PSD $\propto 1/f^{(1+2\alpha)}$.

The power-law index α is a good discriminator between variable stars and quasars†
(Schmidt *et al.* 2010; Butler & Bloom 2011). The key insight is that for time lags below
a year or so quasars have a much steeper structure function ($\alpha \sim 0.4 - 0.5$) than most
variable stars. In other words, compared to their variability at a time lag of, say, one year,
quasars vary by 1-2 orders of magnitude less at time lags below a month or so – this is
not true for the overwhelming majority of variable stars. For UV-excess selected objects,
variability-based methods that utilize α select quasars with a completeness of 90% and a
purity of 95% (Schmidt *et al.* 2010). Furthermore, this performance level is maintained
in the redshift range $2.5 < z < 3$ where color selection is known to be problematic.

The power-law dependence of the structure function for quasar variability cannot be
extrapolated beyond a few years, as shown using SDSS and POSS data by Ivezić *et al.*
(2003) and later using also Stripe 82 data by MacLeod *et al.* (2012). It has been demon-
strated that quasar variability can be statistically described using a stochastic model
called damped random walk (Kelly, Bechtold & Siemiginowska 2009; Kozłowski *et al.*
2010, MacLeod *et al.* 2010, 2011, 2012; Zu *et al.* 2012). Also known in the physics liter-
ature as the Ornstein–Uhlenbeck process, and as the continuous autoregressive process
in the statistics literature, this model includes three parameters: the mean value (of the
quasar magnitude), the characteristic time scale τ, and the asymptotic (at time scales
longer than τ) root-mean-square variability, SF_∞. Alternatively, the model (as well as
its modifications) can be described via a covariance matrix (see MacLeod *et al.* 2010).
The predicted structure function for the damped random walk process is $\mathrm{SF}(\Delta t) = \mathrm{SF}_\infty \left[1 - \exp(-\Delta t/\tau)\right]^{1/2}$. At small time lags, $\mathrm{SF}(\Delta t) \propto \Delta t^{1/2}$, and thus a damped ran-
dom walk is equivalent to an ordinary random walk for $\Delta t < \tau$ (for a random walk,
$\mathrm{PSD} \propto 1/f^2$; the "damped" aspect manifests itself as a flat PSD for $\Delta t > \tau$).

The time span of SDSS data from Stripe 82 is sufficiently long to constrain τ for the
majority of the $\sim$10,000 quasars with light curves (see left panel in Figure 2). MacLeod
et al. (2011) showed that this additional time scale information can be used to improve
significantly the selection based only on the slope of the structure function for small time
lags. For example, it is possible to construct samples with only 15% stellar contamination
even when using *only* variability-based constraints, and 2% stellar contamination when a
UV-excess constraint is added (see Figure 12 in MacLeod *et al.* 2011), while maintaining
a completeness of 90%.

3. Finding quasars with LSST

The last decade has seen fascinating observational progress in optical imaging surveys.
The SDSS dataset is currently being greatly extended by the ongoing surveys such as
Pan-STARRS (Kaiser *et al.* 2010) and the Dark Energy Survey (Flaugher 2008). The
Large Synoptic Survey Telescope (LSST; for a brief overview see Ivezić *et al.* 2008) is
the most ambitious survey currently planned in the visible band. The unparalleled LSST
survey power is due to its large étendue (see Figure 3).

LSST will extend the faint limit of SDSS by about 5 magnitudes and will have unique
survey capability in the faint time domain. In particular, LSST will revolutionize our
understanding of the growth of supermassive black holes with cosmic time, AGN fueling
mechanisms, the detailed physics of accretion disks, the contribution of AGN feedback
to galaxy evolution, the cosmic dark ages, and gravitational lensing (for a detailed dis-
cussion, see Chapter 10 in the LSST Science Book, Abell *et al.* 2009).

---

† This parameter is also a good discriminator of various models for the origin of quasar
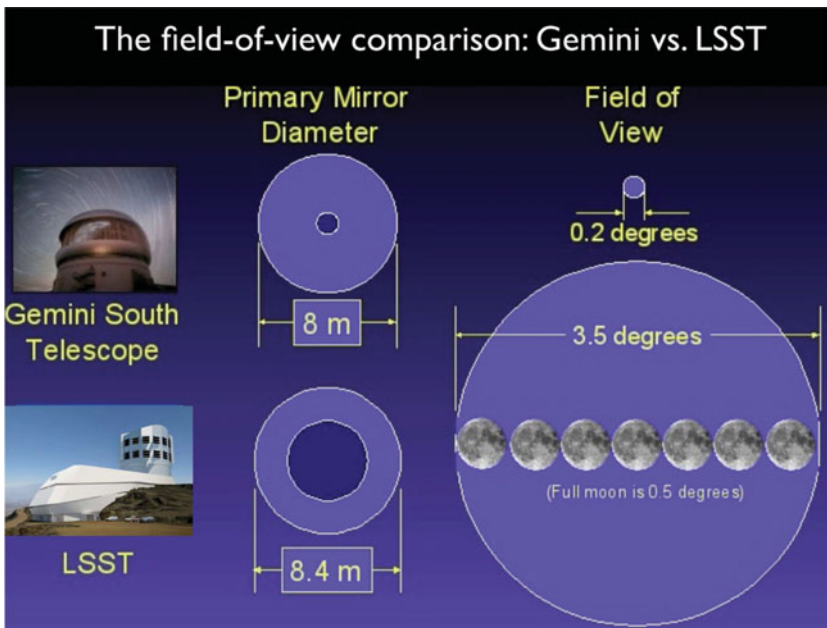variability, see Kawaguchi *et al.* (1998).

Figure 3. A comparison of the primary mirror size and the field-of-view size for LSST and Gemini South telescopes. The product of the primary mirror size and the field-of-view size, the so-called étendue (or grasp), a characteristic that determines the speed at which a system can survey a given sky area to a given flux limit, is much larger for LSST. Figure courtesy of Chuck Claver.

While no massive spectroscopic followup of quasar candidates will be attempted as part of the LSST project, the time-resolved aspect of LSST photometric and astrometric data will enable significant improvements in the completeness and efficiency of resulting quasar samples compared to single-epoch measurements. We first briefly describe anticipated LSST surveys and then discuss how these data will be used to construct quasar samples with up to about 10 million objects.

3.1. *Brief overview of anticipated LSST surveys*

.

The LSST design is driven by four main science themes: probing dark energy and dark matter, taking an inventory of the Solar System, exploring the transient optical sky, and mapping the Milky Way. LSST will be a large, wide-field ground-based system designed to obtain multiple images covering the sky that is visible from Cerro Pachón in Northern Chile. The project is scheduled to have first light around 2019 and the beginning of survey operations by 2021.

The system design, with an 8.4m (6.5m effective) primary mirror, a 9.6 deg^2 field of view, and a 3.2 Gigapixel camera, will allow about 10,000 deg^2 of sky to be covered using pairs of 15-second exposures in two photometric bands every three nights on average, with typical 5σ depth for point sources of $r \sim 24.5$. The system is designed to yield high image quality as well as superb astrometric and photometric accuracy. The survey area will include 30,000 deg^2 with $\delta < +34.5°$, and will be imaged multiple times in six bands, $ugrizy$, covering the wavelength range 320–1050 nm. About 90% of the observing time will be devoted to a deep-wide-fast survey mode which will observe an 18,000 deg^2 region over 800 times (summed over all six bands) during the anticipated 10 years of operations, and yield a coadded map to $r \sim 27.5$. These data will result in databases including about

20 billion galaxies and a similar number of stars, and will serve the majority of science programs. The remaining 10% of the observing time will be allocated to special programs such as a Very Deep and Fast time-domain survey. More details about various science programs that will be enabled by LSST data can be found in the LSST Science Book (Abell *et al.* 2009).

3.2. *Color and variability selection of quasars*

The existing selection algorithms based on colors and photometric variability developed with the aid of SDSS data will be applicable to LSST data, too. Although LSST will not obtain simultaneous multi-band photometry like SDSS did, the averaging of many observations (ranging from about 50-60 in the u band to 180-190 in the r and i bands) will result in sufficiently precise color measurements to recognize easily color offsets from the main stellar locus. The addition of variability information will boost the sample efficiency to levels comparable to those obtained for spectroscopic samples. Two additional selection methods, enabled by the multi-epoch LSST imaging and described below, will further improve the resulting samples.

Detailed simulations of the quasar luminosity function and light curves, the LSST observing cadence, and the LSST photometric error distribution (Abell *et al.* 2009; MacLeod *et al.* 2011; Palanque-Delabrouille et al. 2013) show that the LSST quasar sample will include close to 10 million objects, and will be complete for $M < -23$ objects (a formal absolute magnitude definition cutoff of quasars) to redshifts beyond 3. Notably, LSST will discover about 1000 quasars with redshifts beyond 7 (using the z-band drop-out technique) which will represent a valuable sample for studying the epoch of reionization.

3.3. *Additional constraints: proper motion and differential chromatic refraction*

In addition to photometry, astrometric measurements can help to distinguish quasars from stars. First, measurable proper motion will reject about 2/3 of all stars, even before any color or photometric variability criteria are applied. LSST proper motion errors will be 0.5 mas/yr for sources with $r = 23$ and 1.0 mas/yr for $r = 24$ (Ivezić *et al.* 2008). Simulations of the proper motion distribution for Milky Way stars (for model description, see Ivezić, Beers & Jurić 2012) indicate that over ∼80% of stars with $r < 23$ and over ∼70% of stars with $r < 24$ will have proper motions three times larger than expected measurement errors (with very little dependence on Galactic coordinates, see Figure 4). These high fractions of rejecteable stars are also expected for various stellar subpopulations, such as brown dwarfs (contaminants for very high-redshift quasar candidates) and white dwarfs (contaminants of $z < 2.2$ candidate samples).

An additional astrometric effect that is sensitive to detailed differences in the spectral energy distributions between quasars and stars is the differential chromatic refraction (DCR). Due to the wavelength dependence of atmospheric refraction, in images astrometrically calibrated using stars, quasars show astrometric offsets in a given bandpass as a function of airmass, and also show astrometric offsets between different bandpasses even at a fixed airmass (if larger than one, of course). As shown in Figure 5 from Kaczmarczik *et al.* (2009), the astrometric offsets of quasars from Stripe 82 between the u and g bands, and between the g and r bands, can be up to about 20 mas (depending on redshift), even for moderate airmass (∼1.1-1.2). The measurement errors for these offsets anticipated for the LSST main survey will be below 3 mas for objects brighter than $r = 22$, about 5 mas for objects with $r \sim 23$, and 10-15 mas for objects with $r \sim 24$. Therefore, the DCR offsets for quasars will represent an additional quantity, indpendent of color, variability and proper motion, to help distinguish quasars from stars.
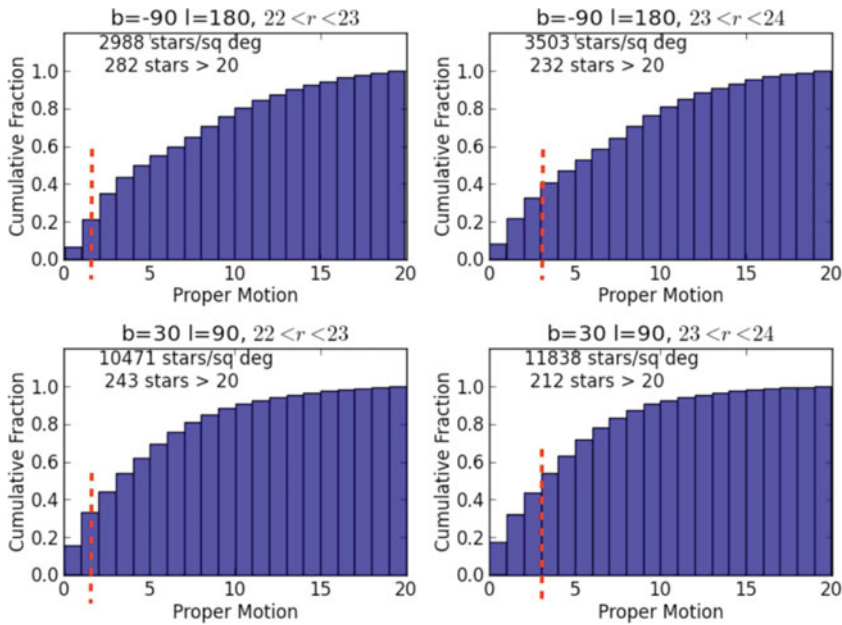
Figure 4. The distributions of proper motions for stars selected from two magnitude bins (left: $22 < r < 23$; right: $23 < r < 24$) and two sky locations (top: south celestial pole; bottom: Galactic longitude $l = 90°$, and latitude $b = 30°$). The vertical dashed lines mark the 3σ cutoffs, where σ is the expected proper motion measurement error for the selected magnitude bins for the main 10-year long LSST survey. The legends in each panel give stellar counts, as well as the counts of stars with anticipated Gaia measurements that provide excellent astrometric calibration. Figure courtesy of Peter Yoachim.

Last but not least, both color and DCR measurements can be used to estimate quasar redshifts with a precision comparable to that expected for LSST galaxies. Using SDSS data, Kaczmarczik *et al.* (2009) obtained a measurement precision for this "photo-astro-z" of 0.03, with the fraction of quasars with redshifts correct to within 0.1 of order 90%.

Acknowledgements

References

Becker, R. H., White, R. L. & Helfand, D. J. 1995, *ApJ*, 450, 559
Bovy, J., Myers, A. D., Hennawi, J., *et al.* 2012, *ApJ*, 749, 41
Butler, N. R. & Bloom, J. S. 2011 *AJ*, 141, 93
Flaugher, B. 2008, In *A Decade of Dark Energy: Spring Symposium, Proceedings of the conferences held May 5-8, 2008 in Baltimore, Maryland. (USA). Ed. by N. Pirzkal & H. Ferguson.*
Hao, L., Strauss, M. A., Fan, X., *et al.* 2005, *AJ*, 129, 1795
Hawkins, M.R.S. & Veron, P. 1995, *MNRAS*, 275, 1102
Ivezić, Ž., Lupton, R. H., Johnston, D. E., *et al.* 2003, ArXiv:*astro-ph/0310566*

Ivezić, Ž., Lupton, R. H., Jurić, M., *et al.* 2004, ArXiv:*astro-ph/0404487*

Ivezić, Ž., Tyson, J. A., Acosta, E., *et al.* 2008, ArXiv:*0805.2366*

Ivezić, Ž., Beers, T. C. & Jurić, M. 2012, *ARAA*, 50, 251

Kaczmarczik, M. C., Richards, G. T., Mehta, S. S. & Schlegel, D. J. 2009, *AJ*, 138, 19

Kaiser, N., Burgett, W., Chambers, K., *et al.* 2010, *Proc. SPIE 7733, Ground-based and Airborne Telescopes III*, vol. 7733, 77330E

Kawaguchi, T., Mineshige, S., Umemura, M., & Turner, E. L. 1998, *ApJ*, 504, 671

Kelly, B. C., Bechtold, J. & Siemiginowska, A. 2009, *ApJ*, 698, 895

Kimball, A., Ivezić, Ž., Wiita, P. J. & Schneider, D. P. 2011, *AJ*, 141, 182

Kozłowski, S., Kochanek, C. S., Udalski, A., *et al.* 2010, *ApJ*, 708, 927

LSST Science Collaboration 2009, LSST Science Book, http://www.lsst.org/lsst/SciBook, arXiv:0912.0201

MacLeod, C. L., Ivezić, Ž., Kochanek, C. S., *et al.* 2010, *ApJ*, 721, 1014

MacLeod, C. L., Brooks, K., Ivezić, Ž., *et al.* 2011, *ApJ*, 728, 26

MacLeod, C. L., Ivezić, Ž., Sesar, B., *et al.* 2012, *ApJ*, 753, 106

Palanque-Delabrouille, N., Yéche, Ch., Myers, A. D., *et al.* 2011, *A&A*, 530, 122

Palanque-Delabrouille, N., Magneville, Ch., Yéche, Ch., *et al.* 2013, *A&A*, 551, 29

Pâris, I., Petitjean, P., Aubourg, É., *et al.* 2012, *A&A*, 548, 66

Richards, G. T., Fan, X., Schneider, D. P., *et al.* 2001, *AJ*, 121, 2308 (see also arXiv:1311.4870)

Richards, G. T., Fan, X., Newberg, H. J., *et al.* 2002, *AJ*, 123, 2945

Richards, G. T., Strauss, M. A., Fan, X., *et al.* 2006, *AJ*, 131, 2766

Richards, G. T., Myers, A. D., Gray, A. G., *et al.* 2009, *ApJS*, 180, 67

Ross, N. P., Myers, A. D., Sheldon, E. S., *et al.* 2012 *ApJS*, 199, 3

Sesar, B., Ivezić, Ž., Lupton, R. H., *et al.* 2007, *AJ*, 134, 2236

Schmidt, K. B., Marshall, P. J., Rix, H.-W., *et al.* 2010, *ApJ*, 714, 1194

Schneider, D. P., Richards, G. T., Hall, P. B., *et al.* 2010, *AJ*, 139, 2360

Strauss, M. A., Weinberg, D. H., Lupton, R. H., *et al.* 2002, *AJ*, 124, 1810

Zakamska, N. L., Strauss, M. A., Krolik, J. H., *et al.* 2003, *AJ*, 126, 2125

Zakamska, N. L., Strauss, M. A., Heckman, T. M., *et al.* 2004, *AJ*, 128, 1002

Zu, Y., Kochanek, C. S., Kozłowski, S. & Udalski, A. 2013, *ApJ*, 765, 106